

Fc Multisite Conjugation and Prolonged Delivery of the Folate-Targeted Drug Conjugate EC140

Yan Zheng,^{||} Hong Cheng,^{||} Sibio Jiang, and Wanyi Tai*



Cite This: <https://doi.org/10.1021/acs.bioconjchem.5c00037>



Read Online

ACCESS |



Metrics & More

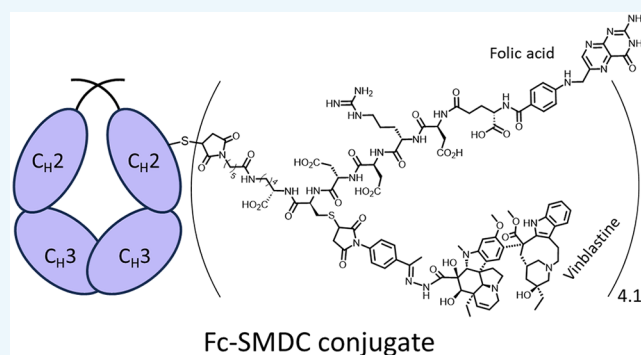


Article Recommendations



Supporting Information

ABSTRACT: Small molecule-drug conjugate (SMDC) is a targeted drug delivery technology that develops in parallel with the antibody-drug conjugate. However, the clinical translation of SMDC faces challenges due to its limited circulating half-life in vivo. The drawback in pharmacokinetics is that it restricts the exposure time of SMDC to tumor tissues and ultimately reduces the therapeutic efficacy. In this study, we chemically conjugated a folate-targeted SMDC EC140 to the long-circulating Fc protein at multiple sites, yielding a stable and high-DAR Fc-SMDC conjugate (Fc-EC140). Fc-EC140 can bear approximately 4 molecules of EC140 per Fc protein (drug-antibody ratio = 4.1) and display enhanced potency in folate receptor (FR)-positive tumor cells compared to the SMDC comparator. In addition, Fc-EC140 retains the FcRn-mediated recycling function and displays an extended half-life of 28 h in the mice. In vivo, antitumor experiments demonstrate that intravenous administration of Fc-EC140 (Q7D \times 3 at a dose of 15 mg/kg) nearly cures the KB tumors, which is far more effective than the comparator EC140 administrated at equivalent doses. This study presents a new strategy for the targeted delivery of SMDC.



INTRODUCTION

Small molecule-drug conjugate (SMDC) is a type of targeted delivery system that consists of a small-molecule targeting ligand, a therapeutic payload, and a linker to join two components together.¹ In the principle of SMDC therapy, the tumor-selective ligand carries the cytotoxic payload to tumor cells and achieves a regional exposure of high drug concentration in tumor sites, leading to the chemotoxic stress in the neoplastic tissue.² SMDC closely resembles its comparator antibody-drug conjugate (ADC) in terms of the delivery strategy and mechanism of action.^{3,4} Therefore, they share many commonalities in the linker design, payload selection, and the choice of tumor-specific targets, as discussed in the recently published reviews.^{5,6} Along with the tremendous success of ADC in the clinic, SMDC is receiving increasing attention.^{7–10} A number of SMDC candidates have been promoted for evaluation in the clinical tests.^{11–13} Moreover, the popularity of SMDC is not only ascribed to its similarity to ADC in delivery but also the advantages over ADC, for example, the nonimmunogenic nature, the low cost in industrial-scale synthesis, and the small molecular weight which benefits the penetration in solid tumors.^{4,14}

Among all the validated SMDCs, the folate-based SMDC that targets the folate receptor (FR) shows significant clinical potential, as evidenced by the number of FR-targeting SMDCs entering clinical trials.^{1,2} This potential is largely owing to two key factors: first, FA binds to the FR with an affinity as low as 1

nM (K_D), ensuring that SMDC can achieve high targetability to tumor cells. Its affinity is comparable to that of antibodies used in the clinic. Second, the FR is highly expressed in various tumor tissues. In contrast, its expression is minimal in normal tissues.^{15–17} The proof of concept that FR acts as a tumor target for chemotherapy has been bolstered by the approval of ADC mirvetuximab soravtansine-gynx (Elahere) for FR-alpha positive ovarian cancer in 2023.¹⁸ As early as two decades ago, Endocyte Inc. has already led to the development of the folate-vincristine alkaloid conjugate, identified as EC140 and EC145 (Vintafolide).^{19–21} These SMDCs utilize FA as the targeting ligand, the hydrophilic peptide (Asp-Arg-Asp-Asp) as spacer, and subsequently conjugates to desacetylvincristine monohydrazone (DAVLBH) via the cleavable bond. Both SMDCs demonstrate the ability to induce cell death in KB cells in a concentration-dependent manner, exhibiting an IC_{50} as low as 11 nM.²² In vivo, EC145 is more active than EC140 in treating established subcutaneous tumors, featuring more durable activity and complete regression of tumors.²⁰ EC145 was

Received: January 26, 2025

Revised: March 22, 2025

Accepted: March 25, 2025

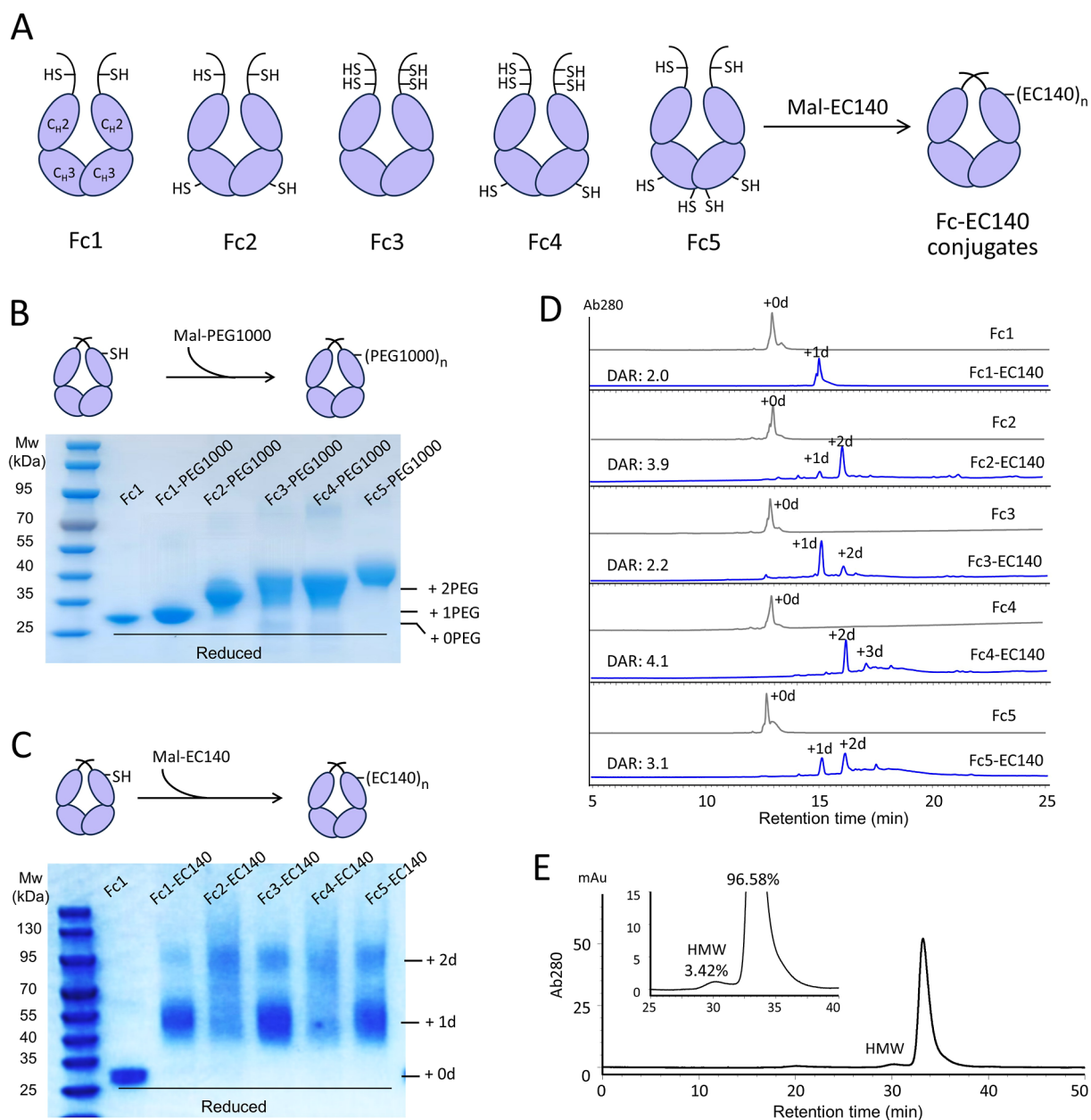


Figure 2. Conjugation of SMDC to Fc protein at multiple sites. (A) The structures of Fc variants and the positions of thiol groups available for EC140 conjugation. The thiol groups come from either the reduced inherent disulfide bonds or the engineered cysteines. (B) The reduced SDS-PAGE to monitor the coupling of Mal-PEG1000 and Fc variants. (C) The conjugation of Mal-EC140 to Fc variants. (D) RP-HPLC analysis of Fc-EC140 conjugates under reducing conditions to determine the DAR distribution. The drug number appendant on each Fc chain (Fc is dimer) is annotated as +0d, +1d, +2d, and +3d. (E) The size exclusion chromatography (SEC) profiling of Fc-EC140 on a TSKgel SuperSW mAb HR column. The percentage of high molecular weight (HMW) is marked on the peak representing the protein aggregates.

with Fc (Figure 1). Here, we choose EC140, rather than EC145 as the model SMDC due to the relatively better stability of the acylhydrazone linker (EC140) over the disulfide EC145.³⁰ By leveraging the advantageous properties of highly water-soluble EC140, we successfully increase the DAR of SMDC-Fc (Fc-EC140) to 4.1. The high-DAR Fc conjugate retains the FcRn-mediated recycling function and displays an extended half-life of 28 h in mice. This Fc strategy significantly enhances the therapeutic potential of EC140 in vivo.

RESULTS AND DISCUSSION

Synthesis and Characterization of the Conjugatable EC140. To conjugate Fc variants, a maleimide (Mal)

functional group is introduced into the structure of EC140. The synthesis of EC140 was conducted following a route previously reported (Scheme 1).²² Briefly, the spacer peptide and folic acid were coupled one by one on the wang resin by using the solid-phase peptide synthesis method. The thiol-containing folate-peptide spacer **5** was cleaved from the resin by TFA and purified by preparative reverse-phase high-performance liquid chromatography (RP-HPLC). The lyophilized powder was condensed with DAVLBH (**6**) in a near quantitative yield to produce the EC140. To introduce a handle for maleimide functionalization, a lysine is appended at the C-terminus of the spacer peptide. A reactive maleimide molecule 6-maleimidohexanoic acid *N*-hydroxysuccinimide

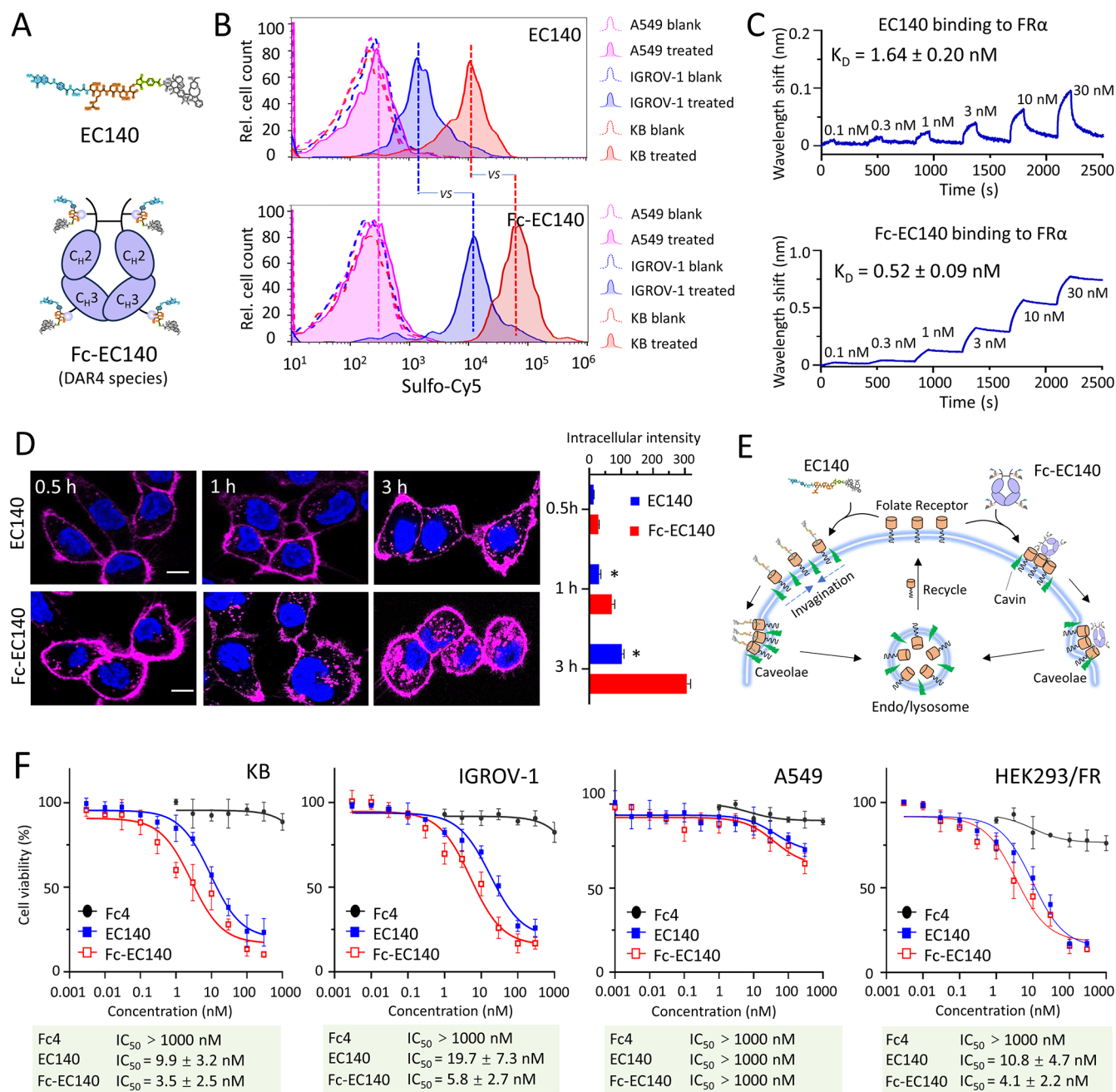


Figure 3. Multivalency by Fc augments the binding, internalization, and cellular potency of EC140. (A) The schematic graphs illustrating the monovalent EC140 and multivalent Fc-EC140 (DAR4). (B) The binding assay of conjugates to KB cells (FR+), IGROV-1 cells (FR+), and A549 cells (FR-) by flow cytometry. The untreated blank cells (dashed-line histogram) are used as controls. (C) Step-binding assay to determine K_D values using BLI. (D) Confocal images of the conjugates' trafficking in KB cells over time. The cell nucleus is counterstained by Hoechst 33,342. Scale bar, 10 μ m. The grouped bar chart on right showing the intracellular fluorescence in cells treated by EC140 and Fc-EC140. * $P < 0.05$. (E) A scheme illustrating the FR-mediated potocytosis with monovalent and multivalent EC140. (F) Cell viability profiling of Fc4, EC140, and Fc-EC140 on four cell lines. Data points are shown as mean \pm SD ($n = 3$).

ester (mc-OSu) finally blocks the lysine residue to generate an extended functional handle for Fc grafting. The final product is confirmed by RP-HPLC and electrospray ionization mass spectrometry (Figure S1).

Multisite Conjugation on Fc Variants. The thiol-maleimide reaction is the most popular chemistry to conjugate drugs to antibodies.^{31–33} The reactive thiol groups could either come from the inherent disulfide bonds of the antibody or the mutant cysteines, known as the THIOMAB approach.³⁴ In the case of natural Fc protein (Fc3 variant), two interchain

disulfide linkages are present in the hinge region. Once reduced, it contains 4 thiol sites for EC140 grafting. Besides the inherent cysteines in the hinge region, other cysteine sites are mutated at the F404 site and/or the C-terminus to enable multisite conjugation. We select the F404 site due to its distance from the FcRn binding site while ensuring adequate surface exposure on the Fc protein.³⁵ This particular site was also utilized in the design of STRO-002, an ADC currently in clinical trial phase I, and has shown no adverse effects on the antibody's functionality.³⁶ Additionally, we opt to introduce a

cysteine at the C-terminus of the heavy chain, which presents less steric hindrance and may facilitate conjugation. Altogether, we finally design five Fc variants with tunable numbers of conjugation sites, termed Fc1, Fc2, Fc3, Fc4, and Fc5 (Figure 2A). All the Fc variants are expressed in the bacterial system to avoid the glycosylation, which can deactivate some effector functions, such as ADCC, ADCP, and CDC, and minimize the effector-mediated toxicity.^{37,38} Their preparation and processing procedures are shown in Figure S2.

We first used Mal-PEG1000 as a model Mal-coupler and incubated it with the reduced Fc in PBS buffer for 3 h at room temperature. The SDS-PAGE image in Figure 2B reveals that all Fc variants are reactive to Mal-PEG1000, but yield quite different DARs. For example, Fc4 and Fc5 likely generate higher DAR species than other Fc variants. The Fc variants were then activated and subsequently incubated with Mal-EC140 to test their grafting efficiency (Figure 2C). SDS-PAGE image shows that all Fc variants can be grafted by either one or two SMDC drugs per chain, but the product bands are a little bit smeared, and their apparent molecular weight is much larger than expected. This discrepancy may be attributed to the impact of SMDC on the band migration. To better illustrate the DAR distribution of all five conjugates, we analyze the products using the reduced RP-HPLC method.³⁹ As shown in the chromatogram (Figure 2D), all Fc conjugates have a retention time longer than that of the unconjugated Fcs. Both Fc2 and Fc3 possess four cysteine sites, but the Fc2 conjugate generates more high DAR species than the Fc3 variant, likely due to the high reactivity of F404C. Fc3 possesses 2 more cysteine sites for conjugation than Fc1, but they produce the similar DAR values. The result indicates that cysteines in the hinge region are only accessible by two SMDCs, despite the low steric hindrance of N-termini.^{40,41} Fc5, which incorporates a cysteine residue at the C-terminus, demonstrates an inefficient conjugation. It might be attributed to the tendency to form the interchain disulfide bond in the region.

Among the Fc variants, Fc4 exhibits the highest coupling efficiency and is successfully paired with an average of approximately four molecules of EC140 per Fc protein (average 2 SMDC per chain, DAR 4.1). Based on the grafting results from other Fc variants, we speculate that the 4 SMDC molecules are conjugated with two cysteines from F404C and two from the hinge region, respectively. Regarding the unreacted thiol groups in the hinge region, we envision that they would self-cross into disulfide bonds, which may enhance structural stability. As a result, the conjugate of EC140 and Fc4, assigned as Fc-EC140, is selected for further investigation in this study. To assess the stability of Fc-EC140 in PBS, SEC was performed to characterize protein aggregation. Figure 2E indicates that the resulting Fc-EC140 is nearly homogeneous and free from aggregation despite the enlarged graph showing a minimal high molecular weight species (HMW, 3.42%). The hydrophilic feature of SMDC EC140 may alleviate the impact of payloads on the stability of Fc proteins. These findings demonstrate that EC140 can be site-specifically conjugated to the Fc4 domain and produce a Fc-EC140 with a high DAR value and a high degree of homogeneity.

Biological Function and Cellular Activity after SMDC Multivalency. To evaluate the effect of Fc multisite conjugation on the potency of EC140, we initially examined the binding selectivity of Fc-EC140 to FR-positive (FR+) KB cells, IGROV-1 cells, and FR-negative (FR-) A549 cells (Figure 3A). The flow cytometry in Figure 3B demonstrates

that Fc-EC140 can bind effectively to the FR-positive cell lines KB and IGROV-1. Moreover, the fluorescence intensity of cell populations shifts along with the FR expression level of treated cells, indicating the selectivity of Fc-EC140 to FR receptors. It is worth noting that the cells treated by Fc-EC140 show much higher mean fluorescence intensity than cells treated by EC140. The augment of affinity is likely owing to the multivalent effect of Fc-EC140 because each EC140 molecule contains one folic acid ligand and Fc conjugate carries more than 4 EC140 molecules on average. To quantitatively evaluate the binding ability, the dissociation constant (K_D) of the conjugates to the folate alpha receptor (FR α) was measured using a bilayer interferometry (BLI) assay (Figure 3C). It shows that Fc-EC140 ($K_D = 0.52 \pm 0.09$ nM) has a much higher binding affinity to FR α than EC140 ($K_D = 1.64 \pm 0.20$ nM). We then assess the intracellular trafficking of conjugates in KB at 37 °C over time. The images in Figure 3D reveal that the cellular uptake is time-dependent. Moreover, it is interesting to find that the internalization of multivalent SMDC (Fc-EC140) is more efficient than the monovalent EC140. The increment in internalization is likely related to the nonclassical lipid raft-mediated endocytosis pathway of folate receptor, namely potocytosis.⁴² The multivalent Fc-EC140 promotes the invagination process and facilitates the formation of caveolae complex, which favors endocytosis (Figure 3E).⁴³ It is worth noting that this result is inconsistent with the previous report from Bandara et al. which concludes that FR clustering has no impact on the internalization rate.⁴⁴ The discrepancy between the results might be attributed to the difference in multivalent conjugates used in the two studies (Fc-SMDC versus multifolate derivatized nanoparticles), and a follow-up study is encouraged to clarify the mechanism.

Encouraged by these promising results, we proceeded to evaluate the antiproliferation effect of Fc-EC140 against FR-positive cancer cell lines. As illustrated in Figure 3F (left panel), both EC140 and Fc-EC140 demonstrate impressive potency, showing at least a 100-fold superiority over Fc ($IC_{50} > 1000$ nM). Notably, Fc-EC140 exhibits approximately 3-fold enhancement in potency compared to EC140. The enhanced potency might be attributed to the high affinity to tumor cells and the corresponding higher payload per molecule after the multivalency by Fc. It is also noted that Fc-EC140 is also highly active in the IGROV-1 cell line, despite its FR expression level being low and its response to EC140 being only moderate (Figure 3F, second panel). Another cell line, A549, which does not express the FR receptor, showed no response to Fc-EC140 (Figure 3F, third panel). We also generated FR-positive cell lines by employing CRISPR-Cas9-mediated knock-in of the FR α gene along with a GFP reporter gene in HEK293 cells. This stable cell line, designated HEK293/FR, has the same genetic background as the original HEK293 cell line but FR α is overexpressed.²⁹ The finding from the stable cell line HEK293/FR is in line with the cytotoxic result observed on other FR-positive cell lines, as depicted in Figure 3F (right panel). Collectively, these results suggest that Fc-EC140 is biologically more active than SMDC EC140, likely owing to the multivalent effect.

In Vivo Activity. Our interest in Fc-EC140 extends to explore whether Fc can improve the pharmacokinetics of EC140 in vivo. We administered fluorescently labeled bioconjugates intravenously to the nude mice implanted with the KB xenograft. The biodistribution of sulfo-Cy5.5-labeled conjugates was monitored using near-infrared (NIR) imaging,

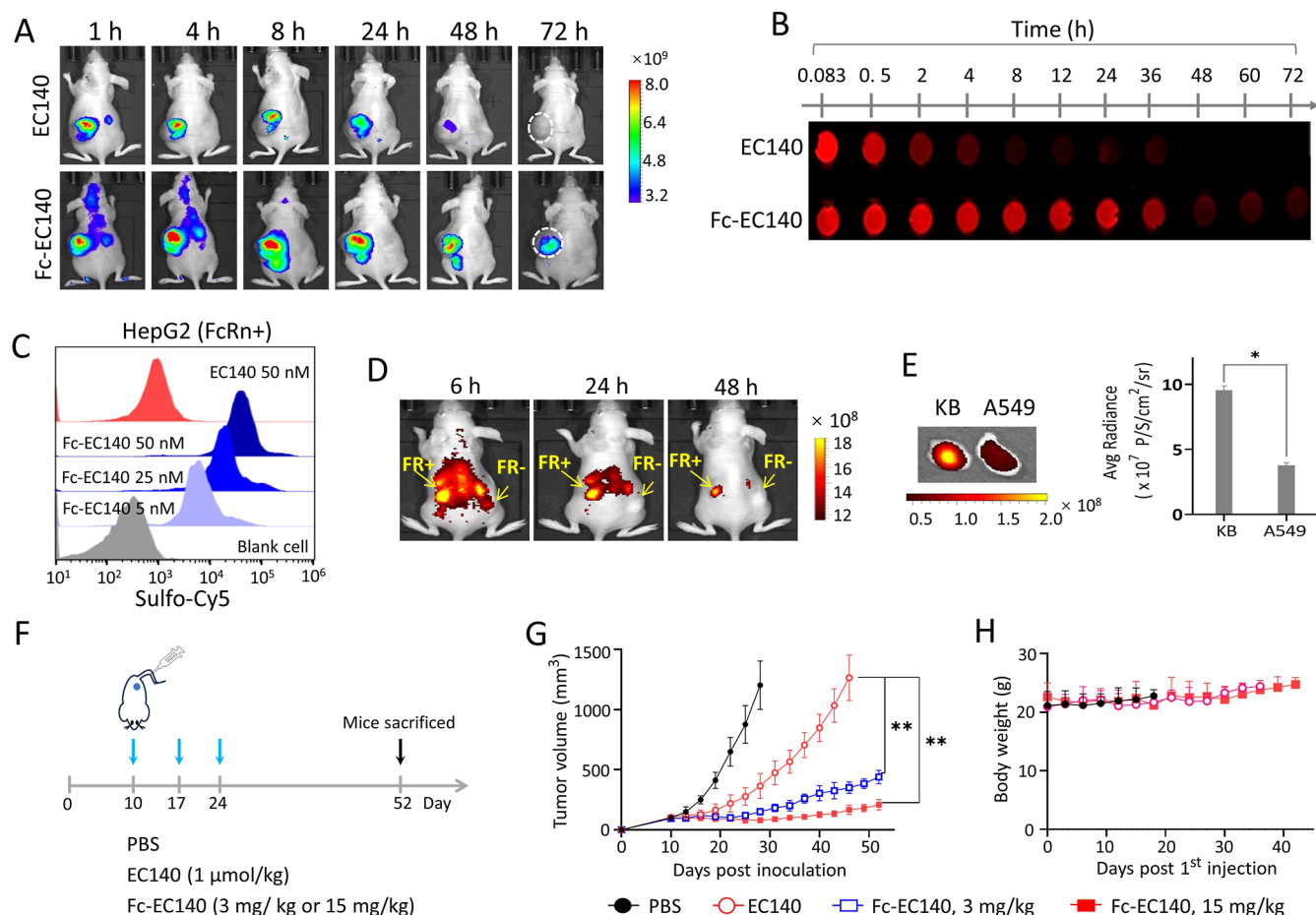


Figure 4. (A) NIR fluorescence imaging to compare the biodistribution of EC140 and Fc-EC140 in the KB tumor-bearing mice. The positions of tumors are circled by the white dashed lines. (B) Pharmacokinetics of EC140 and Fc-EC140 in mice after a single administration at equal doses. The conjugates are labeled with the NIR dye sulfo-Cy5.5, and the red color represents the fluorescent signal of the conjugates. (C) The recognition of FcRn receptors by Fc-EC140 is tested in HepG2 cells (FcRn+) at pH 6.0, in comparison to EC140. (D) A comparison of Fc-EC140 targetability to KB tumor (left dorsal) and A549 tumor (right dorsal) in one mouse. (E) Quantitative analysis of the average radiant efficiency in tumors. Data are presented as mean \pm SD ($n = 3$), $*P < 0.05$. (F) The dose regimen of antitumor experiments. (G) The tumor growth curves after treatment by EC140, Fc-EC140, and PBS control. (H) The body-weight fluctuation in the antitumor experiment. All data are shown as mean \pm SD ($n = 5$), $**P < 0.01$.

as shown in Figure 4A. Our findings reveal that both conjugates accumulate in tumors within 1 h after administration. Notably, the accumulation of Fc-EC140 at the tumor site peaks 4 h after administration, with an average radiant efficiency approximately twice that of EC140, as indicated by region of interest analysis (Figure S3). Furthermore, the strong fluorescent signal persists for at least 72 h in tumors treated by EC140-Fc4. In contrast, the fluorescence of EC140 in the tumor diminishes after the first hour and ultimately becomes undetectable. The disparity in distribution may be attributed to the pharmacokinetics (PK) difference between the two conjugates. We subsequently evaluated the PK of Fc-EC140 and compared it to that of EC140 (Figure 4B). Blood samples were collected at regular intervals following administration, and the retention of the drug in the bloodstream was analyzed using an Odyssey infrared scanner. Quantitative analysis reveals a rapid decline of EC140 concentrations in plasma, with a half-life of only ~ 0.5 h (Figure S4). In contrast, the half-life of Fc-EC140 is dramatically prolonged ($t_{1/2} \sim 28$ h). This optimized PK profile of Fc-EC140 is likely ascribed to the Fc domain and its IgG recycling effect. To confirm the hypothesis, we incubated the bioconjugates with the FcRn-positive cell line

HepG2 and demonstrated that Fc-EC140 can dose-dependently bind with the FcRn receptor at acidic pH. In contrast, EC140 is unable to be recognized by HepG2 cells (Figure 4C).

To evaluate the targetability *in vivo*, we administered sulfo-Cy5.5-labeled Fc-EC140 to mice bearing FR+ KB (left dorsal) and FR- A549 (right dorsal) tumors (Figure 4D). NIR imaging demonstrates a much higher accumulation of drugs in KB tumors than in FR- A549 tumors (Figure 4E). After confirmation of tumor selectivity *in vivo*, we set out to evaluate the antitumor effect in the nude mice bearing KB tumors. Treatments were initiated once the tumor reached a size of 100 mm³. Drugs were administered via tail-vein injection on a frequency of once weekly basis and a total of three doses (Figure 4F). In comparison to the fast growth of tumors treated by PBS control, Fc-EC140 dramatically retards the growth of KB tumors even at a dose as low as 3 mg/kg. At an escalated dose regimen of 15 mg/kg (3 injections), Fc-EC140 demonstrates a robust cure to the KB xenograft mode. The antitumor effect reaches the end of the experiment without observation of any tumor recurrence. In parallel, administering the same dose of EC140 (1 μ mol/kg, equivalent to 15 mg/kg Fc-EC140 based on DAVLBH) exhibits only a

weak inhibitory effect on tumor growth (Figure 4G). It is worth noting that the limited efficacy of EC140 we observed in this study is owing to the low dose and few frequencies of administration. In the conventional SMDC practices (10 $\mu\text{mol}/\text{kg}$, once every 2 days, four doses), a profound antitumor efficacy can be achieved.^{20,22} In the whole experiment, no signs of toxicity were noted, as evidenced by the monitoring of clinical signs and fluctuations in body weight (Figure 4H). Overall, our data demonstrate that the multivalent conjugation of EC140 with the Fc domain displays significant improvement of activity in the FR-positive xenograft models.

CONCLUSIONS

In summary, we successfully prolonged the circulating half-life of EC140 by grafting Fc proteins. To achieve a maximal number of payloads per Fc protein, we engineered 5 Fc variants with multiple thiol sites and tested their capability to conjugate EC140. One variant, Fc4, shows the best reactivity to EC140 and achieves a DAR value of approximately 4.1, which is selected as the candidate. The resulting Fc-EC140 demonstrates remarkable stability, outstanding specificity, and efficacy against FR-positive tumor cells both in vitro and in vivo. Overall, this research validates the significant potential of SMDC as therapeutics by grafting it with the long-circulating Fc effector protein. The findings may shed light on the development of SMDC-based therapies and invite a reevaluation of SMDC EC140/EC145.

ASSOCIATED CONTENT

Supporting Information

The Supporting Information is available free of charge at <https://pubs.acs.org/doi/10.1021/acs.bioconjchem.5c00037>.

The supplementary figures; synthetic procedures of all compounds; experimental methods; and additional cited references (PDF)

AUTHOR INFORMATION

Corresponding Author

Wanyi Tai – Department of Pharmaceutical Engineering, School of Pharmaceutical Sciences, Wuhan University, Wuhan, Hubei 430071, China; orcid.org/0000-0003-3589-8263; Email: wanyi-tai@whu.edu.cn

Authors

Yan Zheng – Department of Pharmacy, Zhongnan Hospital of Wuhan University, Wuhan, Hubei 430071, China; Department of Pharmaceutical Engineering, School of Pharmaceutical Sciences, Wuhan University, Wuhan, Hubei 430071, China

Hong Cheng – Department of Pharmacy, Zhongnan Hospital of Wuhan University, Wuhan, Hubei 430071, China

Sibo Jiang – Hunan Provincial Key Laboratory of the Research and Development of Novel Pharmaceutical Preparations, Changsha Medical University, Changsha, Hunan 410219, China

Complete contact information is available at:

<https://pubs.acs.org/doi/10.1021/acs.bioconjchem.5c00037>

Author Contributions

[†]Y.Z. and H.C. contributed equally.

Notes

The authors declare no competing financial interest.

ACKNOWLEDGMENTS

This work was financially supported by the National Key R&D Program of China (grant no. 2021YFA0909900), the National Natural Science Foundation of China (grant no. 82273860), and the Postdoctoral Fellowship Program of CPSF (grant no. GZC20241277).

REFERENCES

- (1) Zhuang, C.; Guan, X.; Ma, H.; Cong, H.; et al. Small molecule-drug conjugates: A novel strategy for cancer-targeted treatment. *Eur. J. Med. Chem.* **2019**, *163*, 883–895.
- (2) Srinivasarao, M.; Galliford, C. V.; Low, P. S. Principles in the design of ligand-targeted cancer therapeutics and imaging agents. *Nat. Rev. Drug Discovery* **2015**, *14* (3), 203–219.
- (3) Casi, G.; Neri, D. Antibody-Drug Conjugates and Small Molecule-Drug Conjugates: Opportunities and Challenges for the Development of Selective Anticancer Cytotoxic Agents. *J. Med. Chem.* **2015**, *58* (22), 8751–8761.
- (4) Zana, A.; Puig-Moreno, C.; Bocci, M.; Gilardoni, E.; et al. A Comparative Analysis of Fibroblast Activation Protein-Targeted Small Molecule-Drug, Antibody-Drug, and Peptide-Drug Conjugates. *Bioconjugate Chem.* **2023**, *34* (7), 1205–1211.
- (5) Wang, T.; Li, M.; Wei, R.; Wang, X.; et al. Small Molecule-Drug Conjugates Emerge as a New Promising Approach for Cancer Treatment. *Mol. Pharmaceutics* **2024**, *21* (3), 1038–1055.
- (6) Zhang, J.; Hu, F.; Aras, O.; Chai, Y.; An, F. Small Molecule-Drug Conjugates: Opportunities for the Development of Targeted Anticancer Drugs. *ChemMedChem* **2024**, *19* (11), No. e202300720.
- (7) Cazzamalli, S.; Corso, A. D.; Neri, D. Linker stability influences the anti-tumor activity of acetazolamide-drug conjugates for the therapy of renal cell carcinoma. *J. Controlled Release* **2017**, *246*, 39–45.
- (8) Chen, Q.; Wu, Z.; Zhu, H.; Zhang, X.; et al. A Prostate-Specific Membrane Antigen-Targeting Small Molecule-Drug Conjugate Strategy to Overcome the Hematological Toxicity of Olaparib. *J. Med. Chem.* **2024**, *67* (21), 19586–19611.
- (9) Kularatne, S. A.; Wang, K.; Santhapuram, H. K.; Low, P. S. Prostate-specific membrane antigen targeted imaging and therapy of prostate cancer using a PSMA inhibitor as a homing ligand. *Mol. Pharmaceutics* **2009**, *6* (3), 780–789.
- (10) Marks, I. S.; Gardeen, S. S.; Kurdziel, S. J.; Nicolaou, S. T.; et al. Development of a Small Molecule Tubulysin B Conjugate for Treatment of Carbonic Anhydrase IX Receptor Expressing Cancers. *Mol. Pharmaceutics* **2018**, *15* (6), 2289–2296.
- (11) Whalen, K. A.; White, B. H.; Quinn, J. M.; Kriksciukaite, K.; et al. Targeting the Somatostatin Receptor 2 with the Miniaturized Drug Conjugate, PEN-221: A Potent and Novel Therapeutic for the Treatment of Small Cell Lung Cancer. *Mol. Cancer Ther.* **2019**, *18* (11), 1926–1936.
- (12) White, B. H.; Whalen, K.; Kriksciukaite, K.; Alargova, R.; et al. Discovery of an SSTR2-Targeting Maytansinoid Conjugate (PEN-221) with Potent Activity in Vitro and in Vivo. *J. Med. Chem.* **2019**, *62* (5), 2708–2719.
- (13) Peethambaram, P. P.; Hartmann, L. C.; Jonker, D. J.; de Jonge, M.; et al. A phase I pharmacokinetic and safety analysis of epothilone folate (BMS-753493), a folate receptor targeted chemotherapeutic agent in humans with advanced solid tumors. *Invest. New Drugs* **2015**, *33* (2), 321–331.
- (14) Cazzamalli, S.; Dal Corso, A.; Widmayer, F.; Neri, D. Chemically Defined Antibody- and Small Molecule-Drug Conjugates for in Vivo Tumor Targeting Applications: A Comparative Analysis. *J. Am. Chem. Soc.* **2018**, *140* (5), 1617–1621.
- (15) Scaranti, M.; Cojocaru, E.; Banerjee, S.; Banerji, U. Exploiting the folate receptor α in oncology. *Nat. Rev. Clin. Oncol.* **2020**, *17* (6), 349–359.
- (16) Xia, W.; Low, P. S. Folate-targeted therapies for cancer. *J. Med. Chem.* **2010**, *53* (19), 6811–6824.

- (17) Leamon, C. P.; Vlahov, I. R.; Reddy, J. A.; Vetzal, M.; et al. Folate-vinca alkaloid conjugates for cancer therapy: a structure-activity relationship. *Bioconjugate Chem.* **2014**, *25* (3), 560–568.
- (18) Heo, Y. A. Mirvetuximab Soravtansine: First Approval. *Drugs* **2023**, *83* (3), 265–273.
- (19) Reddy, J. A.; Dorton, R.; Westrick, E.; Dawson, A.; et al. Preclinical evaluation of EC145, a folate-vinca alkaloid conjugate. *Cancer Res.* **2007**, *67* (9), 4434–4442.
- (20) Leamon, C. P.; Reddy, J. A.; Vlahov, I. R.; Westrick, E.; et al. Comparative preclinical activity of the folate-targeted Vinca alkaloid conjugates EC140 and EC145. *Int. J. Cancer* **2007**, *121* (7), 1585–1592.
- (21) Vlahov, I. R.; Leamon, C. P. Engineering folate-drug conjugates to target cancer: from chemistry to clinic. *Bioconjugate Chem.* **2012**, *23* (7), 1357–1369.
- (22) Leamon, C. P.; Reddy, J. A.; Vlahov, I. R.; Kleindl, P. J.; et al. Synthesis and biological evaluation of EC140: a novel folate-targeted vinca alkaloid conjugate. *Bioconjugate Chem.* **2006**, *17* (5), 1226–1232.
- (23) Naumann, R. W.; Coleman, R. L.; Burger, R. A.; Sausville, E. A.; et al. PRECEDENT: a randomized phase II trial comparing vintafolide (EC145) and pegylated liposomal doxorubicin (PLD) in combination versus PLD alone in patients with platinum-resistant ovarian cancer. *J. Clin. Oncol.* **2013**, *31* (35), 4400–4406.
- (24) Wang, Z.; Meng, F.; Zhong, Z. Emerging targeted drug delivery strategies toward ovarian cancer. *Adv. Drug Delivery Rev.* **2021**, *178*, 113969.
- (25) Li, J.; Sausville, E. A.; Klein, P. J.; Morgenstern, D.; et al. Clinical pharmacokinetics and exposure-toxicity relationship of a folate-Vinca alkaloid conjugate EC145 in cancer patients. *J. Clin. Pharmacol.* **2009**, *49* (12), 1467–1476.
- (26) Pyzik, M.; Kozicky, L. K.; Gandhi, A. K.; Blumberg, R. S. The therapeutic age of the neonatal Fc receptor. *Nat. Rev. Immunol.* **2023**, *23* (7), 415–432.
- (27) Liu, L. Pharmacokinetics of monoclonal antibodies and Fc-fusion proteins. *Protein Cell* **2018**, *9* (1), 15–32.
- (28) Zheng, Y.; Xu, R.; Chen, S.; Tai, W. In vivo therapeutic effects of small molecule-drug conjugates enhanced by Fc grafting. *Biomaterials* **2022**, *290*, 121820.
- (29) Zheng, Y.; Xu, R.; Cheng, H.; Tai, W. Mono-amino acid linkers enable highly potent small molecule-drug conjugates by conditional release. *Mol. Ther.* **2024**, *32* (4), 1048–1060.
- (30) Bargh, J. D.; Isidro-Llobet, A.; Parker, J. S.; Spring, D. R. Cleavable linkers in antibody-drug conjugates. *Chem. Soc. Rev.* **2019**, *48* (16), 4361–4374.
- (31) Boos, A.; Most, J.; Cahuzac, H.; Moreira da Silva, L.; et al. Antibody-Vincristine Conjugates as Potent Anticancer Therapeutic Agents. *J. Med. Chem.* **2025**, *68* (1), 695–705.
- (32) Liubomirski, Y.; Tiram, G.; Scomparin, A.; Gnaim, S.; et al. Potent antitumor activity of anti-HER2 antibody-topoisomerase I inhibitor conjugate based on self-immolative dendritic dimeric-linker. *J. Controlled Release* **2024**, *367*, 148–157.
- (33) Nakada, T.; Masuda, T.; Naito, H.; Yoshida, M.; et al. Novel antibody drug conjugates containing exatecan derivative-based cytotoxic payloads. *Bioorg. Med. Chem. Lett.* **2016**, *26* (6), 1542–1545.
- (34) Ohri, R.; Bhakta, S.; Fourie-O'Donohue, A.; dela Cruz-Chuh, J.; et al. High-Throughput Cysteine Scanning To Identify Stable Antibody Conjugation Sites for Maleimide- and Disulfide-Based Linkers. *Bioconjugate Chem.* **2018**, *29* (2), 473–485.
- (35) Zimmerman, E. S.; Heibeck, T. H.; Gill, A.; Li, X.; et al. Production of site-specific antibody-drug conjugates using optimized non-natural amino acids in a cell-free expression system. *Bioconjugate Chem.* **2014**, *25* (2), 351–361.
- (36) Li, X.; Zhou, S.; Abrahams, C. L.; Krimm, S.; et al. Discovery of STRO-002, a Novel Homogeneous ADC Targeting Folate Receptor Alpha, for the Treatment of Ovarian and Endometrial Cancers. *Mol. Cancer Ther.* **2023**, *22* (2), 155–167.
- (37) Wang, H.; Song, J.; Quan, Y.; Liu, J.; Tai, W. Chemically Programmed Fc Protein as Antibody Mimetic to Targeting Carbonic Anhydrase IX. *Bioconjugate Chem.* **2024**, *35* (10), 1459–1467.
- (38) Xu, R.; Zheng, Y.; Tai, W. A single-chain fab derived drug conjugate for HER2 specific delivery. *Biomaterials* **2025**, *313*, 122798.
- (39) Xu, Y.; Jiang, G.; Tran, C.; Li, X.; et al. RP-HPLC DAR Characterization of Site-Specific Antibody Drug Conjugates Produced in a Cell-Free Expression System. *Org. Process Res. Dev.* **2016**, *20* (6), 1034–1043.
- (40) Moritz, B.; Stracke, J. O. Assessment of disulfide and hinge modifications in monoclonal antibodies. *Electrophoresis* **2017**, *38* (6), 769–785.
- (41) Hanson, D. C. Some theoretical considerations regarding the effects of steric hindrance and intrinsic global coupling on the flexibility of Fc-anchored immunoglobulins. *Mol. Immunol.* **1985**, *22* (3), 245–250.
- (42) Cheung, A.; Bax, H. J.; Josephs, D. H.; Ilieva, K. M.; et al. Targeting folate receptor alpha for cancer treatment. *Oncotarget* **2016**, *7* (32), 52553–52574.
- (43) Sabharanjak, S.; Mayor, S. Folate receptor endocytosis and trafficking. *Adv. Drug Delivery Rev.* **2004**, *56* (8), 1099–1109.
- (44) Bandara, N. A.; Hansen, M. J.; Low, P. S. Effect of receptor occupancy on folate receptor internalization. *Mol. Pharmaceutics* **2014**, *11* (3), 1007–1013.